Identifiability properties for inverse problems in medical engineering with observability and optimization issues

Juliette Leblond

Identifiability properties for inverse problems in medical engineering, with observability and optimization issues

Juliette Leblond*

Keywords: Inverse boundary value problems, elliptic partial differential equation, medical engineering, observability, optimization

1 Introduction

We discuss a number of inverse identification problems that arise in medical engineering or in neurosciences for functional or clinical brain analysis purposes, like source recovery or conductivity estimation from boundary data, for electro- and magneto-encephalography (EEG/MEG), or in electrical impedance tomograpahy (EIT).
Maxwell's equations under physical assumptions are to the effect that the electrical potential within the head can be modelled as a solution to some partial differential equation (PDE), in spherical or more general 3-dimensional domains [13]. In particular, the quasi-static assumption (time derivatives of the electromagnetic fields are neglected), the PDE is an elliptic Poisson equation for a variable conductivity that only involves the space variable. For the EEG application, on which we mainly focus, available boundary data are furnished by values of the current flux and the electrical potential (measured by electrodes, see figure 1) on the scalp. From such partial and overdetermined boundary measurements of the current flux and the potential (which may be viewed as input and output of the system), the aim is to identify and to reconstruct:
- non–measured boundary data (EEG cortical mapping step, a Cauchy transmission problem),
- unknown current sources supported within the brain (EEG and MEG, singularities of the potential), that correspond to the primary cerebral current,
- or unknown conductivity coefficients (EIT).
These questions can be stated as identification or observation issues for infinite dimensional systems, of which the electrical potential should be viewed as the state. We consider the two first ones, that are deconvolution issues (as in

*Team APICS, INRIA Sophia Antipolis, BP 93, 06902 Sophia Antipolis Cedex, France, tel.: +33 492 387 876, fax: +33 492 387 858, email: juliette.leblond@inria.fr

automatic control, concerning harmonic identification in frequency domain, in dimension 1, see [4]) and inverse potential problems [12].
For point dipolar source, we review a number of identifiability results related to the EEG inverse problem [8], that we also formulate as observability properties. Algorithmical and numerical aspects will be briefly described, most of them requiring (best constrained quadratic) optimization techniques. Our approach relies on harmonic analysis and function theory (the link with holomorphy comes from harmonicity), as does [14]. Compared to other methods (dipole fitting, MUSIC algorithms, [16]), it has the desired feature of allowing to estimate the number of sources that may be correlated (in time).
The overview of the article is as follows. Some notation and definitions are given in section 2. Models and inverse problems in EEG are discussed in section 3, while section 4 is devoted to a two step resolution scheme, which consists first in data transmission, then in source identification. A conclusion is proposed in section 5.

2 Notation, definitions

We recall the definitions of gradient, divergence and Laplace operators for functions acting on $\mathbb{R}^3$, where the space variable is denoted by $x = (x_1, x_2, x_3)$ and the inner product by "$\cdot$". Recall the gradient and divergence operators, formally defined by:

$$\text{grad } = \nabla = \left(\frac{\partial}{\partial x_1}\,,\ \frac{\partial}{\partial x_2}\,,\ \frac{\partial}{\partial x_3} \right)^t\,,\ \text{div } = \nabla\cdot\,,$$

and Laplace operator:

$$\Delta = \nabla \cdot \nabla = \frac{\partial^2}{\partial {x_1}^2} + \frac{\partial^2}{\partial {x_2}^2} + \frac{\partial^2}{\partial {x_3}^2}\,.$$

(div acts on $\mathbb{R}^3$–valued smooth functions, while grad and Δ act on $\mathbb{R}$–valued ones).
We set $\Omega \subset \mathbb{R}^3$ to be a bounded domain with smooth (say $\mathcal{C}^1$) boundary, and n the unit outer normal vector on $\partial\Omega$. The normal derivative on $\partial\Omega$ is then defined by:

$$\frac{\partial u}{\partial n}(x_b) = \lim_{x \to x_b \in \partial\Omega} \nabla u(x) \cdot n(x_b)\,.$$

Functional Hilbert Lebesgue and Sobolev spaces, L^2 and $W^{1,2}$, are classically defined on Ω or $\partial\Omega$, see e.g. [9], as well as $\mathcal{C}(\bar{\Omega})$.

3 Models, inverse problems in EEG

Maxwell equations

Maxwell equations in electrostatics, under quasi-static assumptions, are to the effect that, if E stands for the electrical field, and $\mathbf{\Psi}$ for the electrical potential

[13] in the head:

$$\nabla \times E = 0 \Rightarrow E = \nabla \mathbf{\Psi} \text{ (Faraday's law)}\,.$$

The brain is a non magnetic medium, while it is subject to an electrical activity represented by the current density $\mathcal{J}$ which satisfies

$$\mathcal{J} = \sigma\, E + \mathbf{J} = \sigma\, \nabla \mathbf{\Psi} + \mathbf{J}\,,$$

if $\mathbf{J}$ stands for the primary cerebral current and σ for the electrical conductivity of the head Ω. Hence,

$$\nabla \cdot \mathcal{J} = 0 \text{ (Ampère's law) } \Rightarrow -\nabla \cdot (\sigma\, \nabla \mathbf{\Psi}) = \nabla \cdot \mathbf{J}\,.$$

Partial differential equation

The electrical potential $\mathbf{\Psi} = \mathbf{\Psi}(x)$ is a function (or distribution) of the space variable $x \in \mathbb{R}^3$ which is solution to the following second order elliptic PDE (to be understood in distribution or variational sense, see section 4):

$$\text{div } (\sigma\, \text{grad}\, \mathbf{\Psi}) = \text{div}\, \mathbf{J} \text{ or } \nabla \cdot (\sigma\, \nabla \mathbf{\Psi}) = \text{div}\, \mathbf{J} \text{ in } \mathbb{R}^3\,, \tag{1}$$

$$\text{whence } \sum_{i=1}^{3} \frac{\partial}{\partial x_i} \left(\sigma\, \frac{\partial \mathbf{\Psi}}{\partial x_i} \right) = \sum_{i=1}^{3} \frac{\partial \mathbf{J}}{\partial x_i} \text{ or } \nabla \sigma \cdot \nabla \mathbf{\Psi} + \sigma\, \Delta \mathbf{\Psi} = \nabla \cdot \mathbf{J}\,,$$

with the substitution $\mathbf{J} \to -\mathbf{J}$, for the function or distribution $\mathbf{J}$ with values in $\mathbb{R}^3$ which models the primary cerebral current supported in $\Omega_0 \subset \Omega \subset \mathbb{R}^3$ corresponding to the brain (also with smooth boundary); note that the source distribution $\text{div}\, \mathbf{J}$ is real-valued (or acts on real-valued functions). In EEG, and in the present work as well, σ is often assumed to be isotropic (real–valued) and piecewise constant whence the above PDE reduces to a set of Laplace–Poisson equations, see section 3. We must assume some smoothness properties to hold true for the related problems to make sense. Observe however that in related EIT issues, σ itself is unknown and is the quantity to be recovered (a question related to Calderón's inverse problem).

Inverse EEG problem

The inverse EEG problem consists in recovering $\mathbf{J}$ (at least its support) in some class of source terms, from available boundary data:

$$\mathbf{u} = \frac{\partial \mathbf{\Psi}}{\partial n} \text{ on } \partial\Omega\,,\ \mathbf{y} = (\mathbf{\Psi}(\gamma_i))^t\ ,\ \gamma_i \in \Gamma \subset \partial\Omega\,,\ i = 1, \cdots, L\,, \tag{2}$$

$\mathbf{u}$ being the given current flux on the scalp $\partial\Omega$, $\mathbf{y}$ the measured (difference of) potential, by L electrodes on the scalp, located at positions γ_i on part of the boundary $\gamma_i \in \Gamma \subset \partial\Omega$, $i = 1, \cdots, L$, such that equation (1) holds true.
The above inverse problem is basically ill–posed, and requires additionnal assumptions concerning $\mathbf{\Psi}$ and $\mathbf{J}$ in order to admit a unique solution. Even

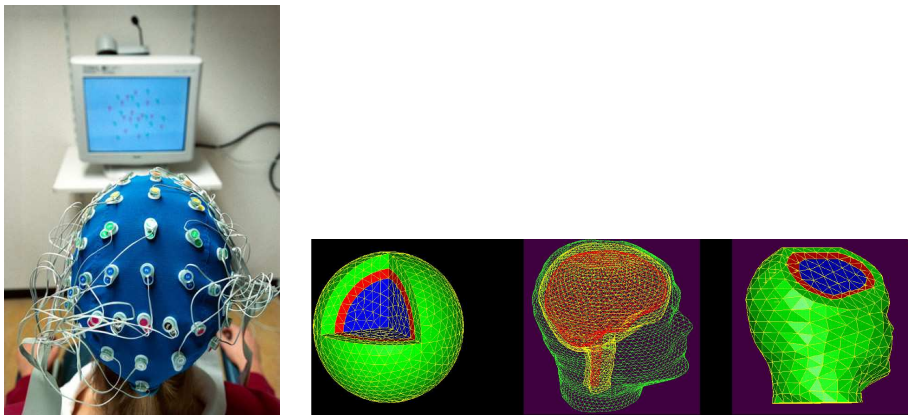

Figure 1: Left (l): measures $\mathbf{u}$ provided by electrodes on the scalp $\partial\Omega$; right (r): head geometries Ω.

then, stability properties of the solution are difficult to ensure, and only hold under further a priori assumptions on the model and the data [12]. These well-posedness aspects will be discussed within the harmonic framework of section 4, having in mind that the available measurements $\mathbf{u}$, $\mathbf{y}$ are practically approximate and incomplete.

Direct EEG problem

Concerning the associated direct problems, the source distribution $\mathbf{J}$ is given, as well as boundary data example of Dirichlet or Neumann type [9]. Dirichlet boundary data consists in being given $\mathbf{\Psi}$, while Neumann data corresponds to $\mathbf{y} = \frac{\partial \mathbf{\Psi}}{\partial n}$, both on the overall $\partial\Omega$. For smooth conductivities, these problems are well–posed, under the following necessary compatibility condition for the second one, for which the solution is unique up to an additive constant:

$$\int_{\partial\Omega} \sigma \, \frac{\partial \mathbf{\Psi}}{\partial n} = 0 \,,$$

with respect to the Lebesgue measure on the surface $\partial\Omega$. In particular, whenever $\mathbf{\Psi}$ (or $\mathbf{y}$) is smooth enough on $\partial\Omega$, then so is $\mathbf{\Psi}$ in Ω which thus admits a continuous trace on $\partial\Omega$. Actually, for smooth or piecewise constant conductivities σ, the assumption $\mathbf{\Psi} \in W^{1,2}(\partial\Omega)$ is enough to ensure that $\mathbf{\Psi} \in \mathcal{C}(\bar{\Omega})$, see e.g. [7] for constant σ.

Observability issues

The electrical potential $\mathbf{\Psi} = \mathbf{\Psi}(x)$, a real valued function (or distribution) of the space variable $x \in \Omega \subset \mathbb{R}^3$ may be viewed as a state variable for the static infinite dimensional state model (1). On the boundary $\partial\Omega$, the current

flux $\mathbf{u}$ corresponds to the associated input, the potential to the output. The inverse source problem consists in finding the state or its singularities, given input/output data $\mathbf{u}$ and $\mathbf{y}$, which is an observability problem (in general, for EEG, $\mathbf{u}$ is assumed to vanish; for EIT, $\mathbf{u} \neq 0$ is applied by electrodes).
It is difficult at that stage to explicit the link between $\mathbf{u}$, $\mathbf{y}$, $\mathbf{\Psi}$ as a consequence of (2), (1) and Green's formula though already:

$$\mathbf{y} = C\,\mathbf{\Psi}_{|\partial\Omega}\,,$$

where C denotes the pointwise evaluation operator at the L points $\gamma_i \in \partial\Omega$ corresponds to an observation operator. With the above smoothness situation, that we now assume to hold true, the linear operator C is continuous in particular in the sense that

$$|\mathbf{y}| \lesssim \|\mathbf{\Psi}\|_{L^\infty(\partial\Omega)} \lesssim \|\mathbf{u}\|_{L^\infty(\partial\Omega)}\,.$$

Note that C has finite dimensional range and is formally defined on those continuous functions on $\partial\Omega$. Without further assumption, the observation of the infinite dimensional state $\mathbf{\Psi}$ with very few boundary conditions is lost in advance. We will see that it goes differently and that some quantities become observable, at least approximately, under some hypotheses.
Similarly, variational formulations of (1) and (2) may be expressed as:

$$\mathbf{u} = K_{\mathbf{J}}\left(\mathbf{\Psi}_{|\partial\Omega}\right),\ \text{where } K_{\mathbf{J}} : \mathbf{\Psi}_{|\partial\Omega} \mapsto \frac{\partial\mathbf{\Psi}}{\partial n}_{|\partial\Omega}\,,$$

for an operator $K_{\mathbf{J}}$ which appears through Green formula, see (4) and (6), the so-called Dirichlet–to–Neumann operator. In the present situation, a preliminary step requires to build $\mathbf{\Psi}$ on $\partial\Omega$ from $\mathbf{y}$, which would not be needed if measurements $\mathbf{y}$ were available as a function on the whole boundary $\partial\Omega$, rather at L points in $\Gamma \subset \partial\Omega$. But this only reinforce the strong ill–posed property of the corresponding inverse observability issue, of building the state $\mathbf{\Psi}$ on Ω from $\mathbf{u}$ and $\mathbf{y}$ on $\partial\Omega$, but unknown $\mathbf{J}$, among solutions to (1), an impossible task. Regularization schemes by constrained optimization (best quadratic approximation) are then used in order to state and to solve these inversion issues in several consecutive steps.

4 EEG inverse source problem

Classically, spherical head models are considered and supposed to be made of 3 spherical homogeneous layers [8]. Put then $\Omega = \mathbb{B}$ unit ball, whence $\partial\Omega = \mathbb{S}$, the unit sphere. Put $\Omega_0 = r_0\,\mathbb{B}$ for some $0 < r_0 < 1$ (brain), Ω_1 (skull), Ω_2 (scalp), such that $\Omega = \Omega_0 \cup \bar{\Omega}_1 \cup \Omega_2$, see figure 2, (l). Let further $\partial\Omega_i = S_{i-1} \cup S_i$ for $i = 1, 2$ and spheres S_i (in particular, $S_0 = \partial\Omega_0$, $S_2 = \partial\Omega$).
The head conductivity σ is assumed to be known and piecewise constant: on Ω_k, $\sigma = \sigma_k > 0$ (with $\sigma_0 = \sigma_2 = 1$ up to a renormalization, and $1/\sigma_1 \in [20, 80]$). Further, because $\mathbb{R}^3 \backslash \bar{\Omega}$ (the air, the neck is ignored) is a non conductive medium, we have that σ vanishes outside Ω.

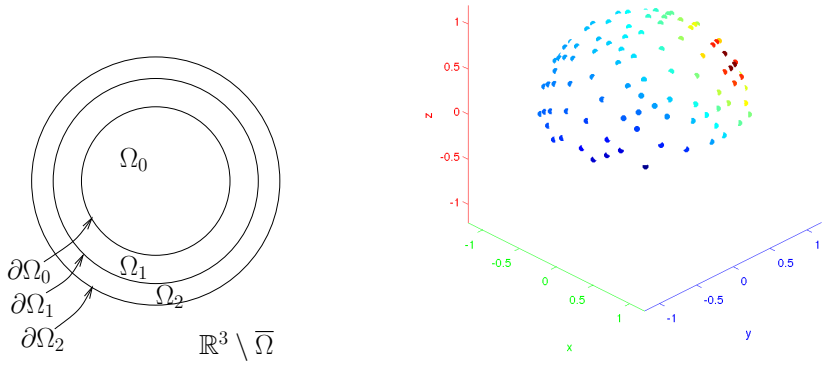

Figure 2: Left (l): 3 layers spherical head model; right (r) : measured values $\mathbf{y} = \mathbf{y}_2$ of $\mathbf{\Psi}$ by $L = 128$ electrodes on the upper part of the scalp.

Given $\mathbf{u}$ and $\mathbf{y}$ on $\partial\Omega$ from (2) (see figure 2, (r)), we thus want to find $\mathbf{J}$ or at least its support, such that $\mathbf{\Psi}$ satisfies (1), under necessary assumptions, needed to ensure well–posedness and observability like properties, see the hypothesis (7) below concerning $\mathbf{J}$. In particular, we want to locate the singularities of $\mathbf{\Psi}$ in Ω_0. More precisely, we get from (1) that:

$$\begin{cases} \Delta\,\mathbf{\Psi} = 0 \text{ in } \left(\mathbb{R}^3 \setminus \bar{\Omega}\right) \cup \Omega_2 \cup \Omega_1\,, \\ \Delta\,\mathbf{\Psi} = \operatorname{div}\mathbf{J} \text{ in } \Omega_0\,, \\ \mathbf{\Psi} \text{ and } \sigma\dfrac{\partial\mathbf{\Psi}}{\partial n} \text{ continuous across } S_i\,,\ i = 0,1,2\,, \end{cases} \tag{3}$$

where the transmission conditions (obtained from Green formula, see (4) below) express the continuity of the potential and of the normal current across the interfaces S_i. We use two main consecutive steps for solving the EEG source inverse problem [8]:
- A first boundary data extension / transmission step (Cauchy type inverse problems), also called "cortical mapping" step in the present framework: the given boundary data are transmitted from $\partial\Omega = S_2$ to S_0, see section 4.1.
- A second source localization step, inside Ω_0 (geometric inverse problems) from the above transmitted data on S_0, see section 4.2, for some class of $\mathbf{J}$.

4.1 Data transmission

Let $S_i^{\pm}$ denote the inner and outer side of S_i, for $i = 0, 1, 2$. From (3), we get in the outermost two layers Ω_i, $i = 1, 2$, with the convention $\sigma_3 = 0$:

$$\begin{cases} \Delta\, \mathbf{\Psi} = 0 \text{ in } \Omega_i\,, i = 1, 2, \\ \\ \mathbf{\Psi}_{|_{S_i^-}} = \mathbf{\Psi}_{|_{S_i^+}}\,, \sigma_i \dfrac{\partial \mathbf{\Psi}}{\partial n}_{|_{S_i^-}} = \sigma_{i+1} \dfrac{\partial \mathbf{\Psi}}{\partial n}_{|_{S_i^+}}\,,\ i = 0, 1, 2. \end{cases}$$

In order to get the Cauchy data on S_0, we thus face two consecutive Cauchy type transmission problems in the spherical shells Ω_i, from their outer boundaries S_i to their inner ones S_{i-1}. Put $\mathbf{y} = \mathbf{y}_2$, $\mathbf{u} = \mathbf{u}_2 = 0$. The first transmission problem is the following. Given $\mathbf{y}_2 \in \mathbb{R}^L$ such that:

$$\begin{cases} \Delta\, \mathbf{\Psi} = 0 \text{ in } \Omega_2\,, \\ \\ (\mathbf{\Psi}(\gamma_i))^t = \mathbf{y}_2 \in \mathbb{R}^L\,,\ \gamma_i \in \Gamma \subset S_2\,,\ i = 1, \cdots, L\,, \\ \\ \dfrac{\partial \mathbf{\Psi}}{\partial n}_{|_{S_2}} = \mathbf{u}_2 = 0\,, \end{cases}$$

get on S_1:

$$\mathbf{y}_1 = \mathbf{\Psi}_{|_{S_1}} \text{ and } \mathbf{u}_1 = \frac{1}{\sigma_1} \frac{\partial \mathbf{\Psi}}{\partial n}_{|_{S_1}}\,,$$

recalling the normalization $\sigma_2 = 1$. Once $\mathbf{u}_1$ and $\mathbf{y}_1$ have been computed on S_1 (either by their pointwise values at points from a mesh or by their spherical harmonics expansions [9]), the second transmission problem in Ω_1 can be stated as follows. Given $\mathbf{u}_1$, $\mathbf{y}_1$ on S_1 such that:

$$\Delta\, \mathbf{\Psi} = 0 \text{ in } \Omega_1\,,\ \mathbf{\Psi}_{|_{S_1}} = \mathbf{y}_1\,,\ \sigma_1 \frac{\partial \mathbf{\Psi}}{\partial n}_{|_{S_1}} = \mathbf{u}_1\,,$$

get on S_0:

$$\mathbf{y}_0 = \mathbf{\Psi}_{|_{S_0}} \text{ and } \mathbf{u}_0 = \sigma_1 \frac{\partial \mathbf{\Psi}}{\partial n}_{|_{S_0}}\,.$$

Cauchy-Holmgren uniqueness result asserts that, for compatible (exact) data, there exists a unique solution to the above transmission problem. Ill-posedness, however, comes from unstability properties of such Cauchy type issues, though sufficient conditions for stability are available [1], [19]. As soon as we turn to experimental (corrupted) data, an exact solution may not even exist. Robust approximate and constructive identifiability / observability can be ensured as follows, by regularization and approximation.
Let E_3 be the radial fundamental solution of Laplace equation in $\mathbb{R}^3$, see [9]:

$$E_3(x) = \frac{1}{4\,\pi |x|}\,,\ \text{which satisfies } \Delta\, E_3 = \delta_0 \text{ on } \mathbb{R}^3\,,$$

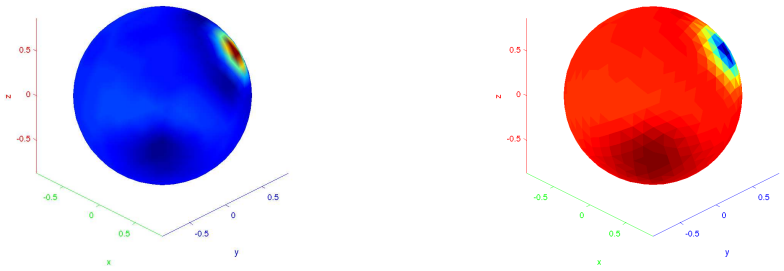

Figure 3: Potential and normal current transmitted on S_0: (l) $\mathbf{y}_0$; (r) $\mathbf{u}_0$.

if δ_C stands for the Dirac distribution (mass) at point C. Using Green formula for harmonic functions, we get that for $y \notin \Omega_i$,

$$\int_{\partial\Omega_i} \left(\mathbf{\Psi}(y) \, \frac{\partial E_3}{\partial n}(x-y) - E_3(x-y) \, \sigma_i \, \frac{\partial \mathbf{\Psi}}{\partial n}(y) \right) dy = 0 \,, \tag{4}$$

where

$$\frac{\partial E_3}{\partial n}(y-x) = \frac{(x-y)\cdot n(x)}{4\,\pi\,|x-y|^3} \,.$$

To handle this cortical mapping step, $\mathbf{\Psi}$, $\frac{\partial \mathbf{\Psi}}{\partial n}$ are discretized on the meshes and represented as a (big) vector Ψ which represents $(\mathbf{u}_i \,,\ \mathbf{y}_i)$ at points on S_i, $i = 0, 1, 2$. We then look for such a Ψ that lies in the kernel of some matrix H, a relation which expresses (4), and such that $M\,\Psi = (\mathbf{u}_2 \,,\ \mathbf{y}_2)$, the given data, for a measurement matrix M. Formula (4) however is solvable only for compatible (exact) data (still the ill-posedness of Cauchy problem), whence we turn to optimization with boundary elements method that consists in minimizing the following discrete criterion on $\partial\Omega_i$ [15]:

$$\min_{H\,\Psi=0} \|M\,\Psi - (\mathbf{u}_2 \,,\ \mathbf{y}_2)\|^2_{l^2} + \lambda \, \|R\,\Psi\|^2_{l^2} \ , \tag{5}$$

for some Lagrange parameter $\lambda > 0$ and an appropriate matrix R which expresses the contsraint (Tykhonov regularization). This furnishes a robust regularized resolution schemes, even for non-compatible data, that we use for numerical purposes, through boundary elements methods used and described in [8]. See figure 2 (electrodes pointwise data $\mathbf{y} = \mathbf{y}_2$ on the scalp $\partial\Omega_2$), and figure 3, which represents the transmitted Cauchy data $\mathbf{y}_0$, $\mathbf{u}_0$ on the cortex $S_0 = \partial\Omega_0$, at 642 points on the meshed spheres, computed using the boundary elements method recalled above. There, and in figures 5, 6 as well, we got direct simulated data with $\mathbf{J}$ as in (7) and $K = 2$ sources $C_1 = (.5, .5, .5)$, $C_2 = (.5, -.5, -.4)$. All the numerical experiments were done using the software FindSources3D (matlab) [11].

Note that related bounded extremal problems (BEP) express a criterion similar to (5), though expressed in $L^2(\partial\Omega_i)$ norm, within Hardy classes of gradients of harmonic functions, see [2]. There, expansions on bases of spherical harmonics may be used rather than pointwise values, for the discretization. In any cases, robust approximate solutions are furnished by approximating the Laplace operator while sticking to the given data (BEM), or approximating the boundary data by harmonic functions (BEP), with a regularizing norm constraint. Note further that formula (4) links $\mathbf{u}_i$, $\mathbf{y}_i$ on S_i to $\mathbf{u}_{i-1} = \frac{\partial \mathbf{\Psi}}{\partial n}$, $\mathbf{y}_{i-1} = \mathbf{\Psi}$ on S_{i-1} for $i = 1, 2$.

4.2 Source identification

From the cortical data $\mathbf{y}_0$, $\mathbf{u}_0$ on S_0, the inverse source problem is now to find the distribution $\mathbf{J}$ or its support inside the ball Ω_0 such that:

$$\begin{cases} \Delta\, \mathbf{\Psi} = \operatorname{div} \mathbf{J} \text{ in } \Omega_0\,, \\ \\ \mathbf{\Psi}_{|_{S_0}} = \mathbf{y}_0\,, \quad \sigma_1 \dfrac{\partial \mathbf{\Psi}}{\partial n}_{|_{S_0}} = \mathbf{u}_0\,. \end{cases}$$

This is still an ill-posed problem which admits infinitely many solutions $\mathbf{J}$ without further assumptions. The potential $\mathbf{\Psi}$ may be expressed in terms of S, by convolution with a fundamental solution of Laplace equation in $\mathbb{R}^3$, see [9]. We thus get:

$$\mathbf{\Psi}(x) = h(x) - \int_{\Omega_0} E_3(x-y) \operatorname{div} \mathbf{J}(y)\, dy$$

$$= h(x) + \int_{\Omega_0} \nabla E_3(x-y) \cdot \mathbf{J}(y)\, dy = h(x) + \mathbf{\Psi}_s(x)\,, \tag{6}$$

for some function h harmonic in Ω_0, where $\mathbf{\Psi}_s$ represents the singular part of $\mathbf{\Psi}$ and contains all information about the source term ($\mathbf{\Psi}_s$ is harmonic outside Ω_0 and vanishes at ∞). It can be computed on S_0 from $\mathbf{u}_0$ and $\mathbf{y}_0$ expanded on the spherical harmonic basis [9].

4.2.1 Pointwise dipolar sources

The following assumption on $\mathbf{J}$ is classical in EEG, which amounts to assume that the potential $\mathbf{\Psi}$ is created by K dipolar sources $C_k \in \Omega_0$ with associated moments $p_k \in \mathbb{R}^3$:

$$\mathbf{J} = \sum_{k=1}^{K} p_k \delta_{C_k}\,, \text{ whence } \Delta\mathbf{\Psi} = \operatorname{div} \mathbf{J} = \sum_{k=1}^{K} p_k \cdot \nabla \delta_{C_k}\,. \tag{7}$$

In this situation, we get (at $x \neq C_k$ in $\mathbb{R}^3$):

$$\mathbf{\Psi}_s(x) = \sum_{k=1}^{K} \frac{p_k \cdot (x - C_k)}{4\,\pi\,|x - C_k|^3}\,.$$

It allows to ensure well-posedness of the above homogeneous inverse source problem, from Dirichlet-Neumann data on $\partial\Omega_0$, as well as the overall identifiability property of the sources from boundary data on $\partial\Omega$ through the consecutive layers, provided that the Dirichlet data $\mathbf{y}_2$ is furnished on an open subset $\Gamma \subset \partial\Omega$ (whenever the potential values are only given at L points $\gamma_i \in \Gamma$, which is practically the case, a first robust interpolation step is required). Uniqueness of $\mathbf{J}$ in the above class, hence of K, p_k, C_k, for $k = 1, \cdots, K$, is established in [10]. Together with available stability properties of the homogeneous pointwise source problem [18], [19], this can still be viewed as an approximate observability property, though this has to be make precise, since there is now $6\,K+1$ quantities to be identified (which may be not that big) from a huge number of data (infinite dimensional, despite the function $\mathbf{\Psi}_s$ defined on S_0 is either expanded as a series or given by poitwise values at the mesh points, for computational purposes).
Again, constructive aspects and robust resolution algorithms form the key points. We explain below the localization algorithm from [3], [8], used by the software FindSources3D [11] for numerical computations. It consists in singularities estimation by best quadratic rational approximation of $\mathbf{\Psi}_s$ (actually, of $\mathbf{\Psi}_s^2$) on the boundaries (circles) of families of plane sections of Ω_0 (disks). Let, for instance, $\Pi = \{(x_1, x_2, x_3)\,,\ x_3 = 0\}$ denote the (x_1, x_2) plane, and $\Pi_p = \{(x_1, x_2, x_3)\,,\ x_3 = 0\}\,,\ x_3 = x_{3p}\}$, with the disk $D_p = \Pi_p \cap \Omega_0$ and the circle $T_p = \partial D_p = \Pi_p \cap S_0$, $p = 1, \cdots, P$, for some integer $P > 0$ (see figure 4).

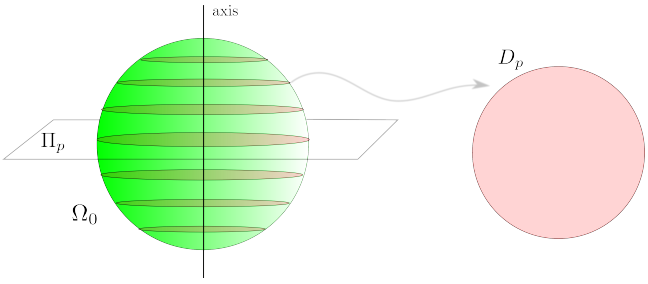

Figure 4: Plane sections Π_p of Ω_0, disks D_p.

From $\mathbf{\Psi}_s$ on S_0, build for $p = 1, \cdots, P$ the complex variable functions f_p such that, for $z = x_1 + i\,x_2 \in T_p$:

$$f_p(z) = \mathbf{\Psi}_s^2(x_1, x_2, x_{3p}) = \left[\sum_{k=1}^{K} \frac{\phi_{kp}(z)}{(z - z_{kp})^{3/2}}\right]^2 ,$$

for functions ϕ_{kp} that are holomorphic in D_p. For each p, f_p coincides on T_p with a function (say f_p) that admits K singularities z_{kp} in D_p due to sources, related to their parameters C_k, p_k (and to x_{3p}^2 as well). Indeed, if we put z_k for the complex affix of C_k in $\Pi \cap S_0$, assuming that $z_k \neq 0$, then:

- the complex arguments of the K singularities (z_{kp}) of f_p do not depend on p and equal the argument of z_k,
- for fixed k, the modulus $|z_{kp}|$ is maximum w.r.t. p in the section D_{p*} closest to (or containing) C_k and $z_{kp*} = z_k$.
This is illustrated in figure 5, for C_1, C_2 as in the numericals of figures 2, 3, with $P = 21$ sections. These considerations allow to reduce the 3D inverse

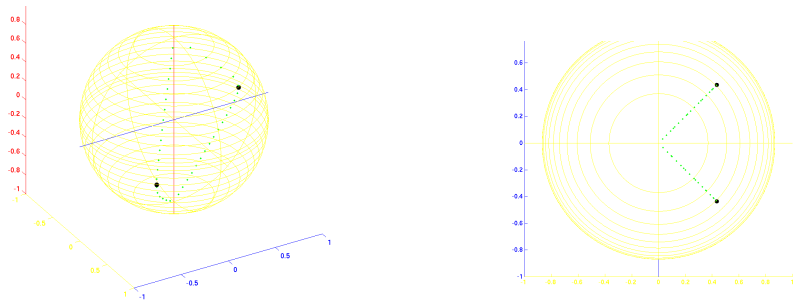

Figure 5: Sources C_k in Ω_0 (big black dots), singularities (z_{kp}) (small green dots), for $k = 1, 2$; left: side view; right: from above (top of x_3 axis).

source problem to a family of P 2D problems that consists, for $p = 1, \cdots, P$, in recovering the singularities $z_{kp} \in D_p$, being given f_p on the boundary T_p.
For fixed p, because $z_{kp} \in D_p$ appears both as triple poles and branchpoints of f_p, they may be approximated by the poles of best constrained quadratic rational approximants to f_p on T_p. The formulation we consider is the following [5]. For $n \geq 0$, find polynomials p_n, q_n with degree $p_n \leq$ degree $q_n \leq n$ and q_n with less than n zeroes in D_p, that minimize

$$\left\| f_p - \frac{p_n}{q_n} \right\|_{L^2(T_p)}$$

among such functions. Solutions p_n/q_n are the best quadratic rational approximants to f_p on T_p of degree n. Their poles in D_p, those zeroes of q_n within D_p, accumulate (in some sense) to the singularities z_{kp} of f_p as n increases, a deep result from potential theory established in [6]. Related resolution schemes are briefly described in [8] again. Hence, computing the zeroes of q_n for suitable values of n allows to efficiently estimate the quantity K of sources and to approximately localize the singularities z_{kp}. Indeed, one first increases the degree n until the value of the approximation criterion (the quadratic error on T_p) is small enough on T_p (or stationary): this furnishes an estimation of K, a nice feature of this scheme. Then, only, for such n, one compute the solution p_n/q_n and its n poles, which are close to z_{kp}. Similarly, one can compute best rational approximants with m triple poles within D_p, represented as rationals $p_{3m}/(q_m)^3$ in the above criterion. It appears that a single triple poles already

approximate well enough the singularities z_{kp}, even for $K = 2$ or more, see figure 6 (and [8, Prop. 1] for the case $K = 1$). The above algorithm can be run

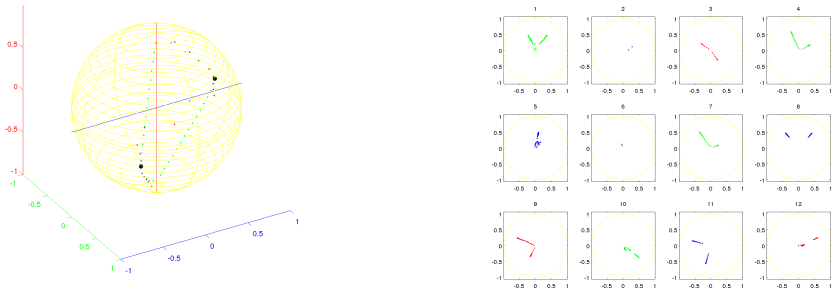

Figure 6: Left: sources C_k in Ω_0 (big black dots), singularities (z_{kp}) (small green dots), for $k = 1, 2$, triple pole (small red dots); right: poles viewed from above, for 12 different planar sections Π.

for several section directions Π. The computed series of poles for varying k, p in each direction will then approximately intersect at C_k, as the series of singularities do, see figure 7. We thus run a clustering algorithm as a last estimation step. For figures 7 and 8, the numerically generated data correspond to $\mathbf{J}$ as in (7) and $K = 2$ sources $C_1 = (.2, .3, .4)$, $C_2 = (-.3, -.2, .4)$ (and moments $p_1 = (0, .2, .6)$, $p_2 = (.1, 0, .8)$). Figures 8 and 9 show actual and estimated sources and moments. In figure 9, direct data from BESA company taken from more realistic geometries (from MRI data, then translated on spheres) have been considered. These numericals illustrate the efficiency of the involved approximate identification schemes (observers?).

5 Conclusion

Concerning geometric inverse problems of singularity localization (they must be sources, defaults, cracks), from boundary data, a source term $\mathbf{J}$ is said to be silent in Ω_0 if it not visible from outside Ω_0, that is if it produces a potential that vanishes there, $\mathbf{\Psi}_0$ on $\mathbb{R}^3 \setminus \bar{\Omega}_0$. Silent (non-observable) sources for the homogeneous EEG inverse problem are currently under study (they are never pointwise).
Similar inverse problems appear related to other physical potentials, solution to Maxwell or Newton equations, with applications in magnetoencephalography (MEG), magnetization, geodesy.
Taking the time variable into account should be done for the present EEG model, which would allow to make use of infinite-dimensional linear system theory [17].
Concerning EIT issues, using the normal current $\mathbf{u}$ applied by electrodes on the scalp as an effective control is rather appealing, and especially looking for some

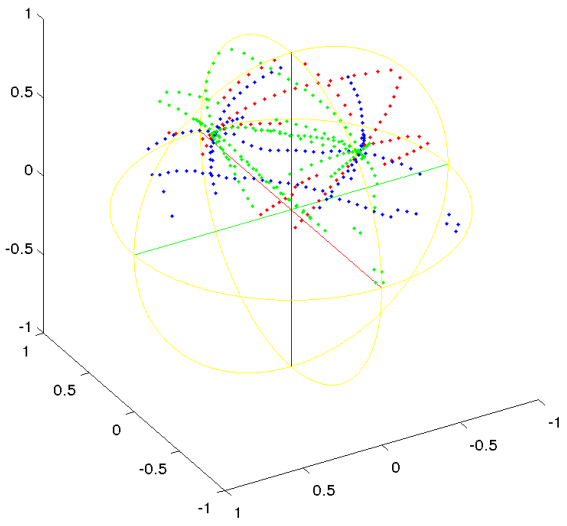

Figure 7: Superposition of estimated poles in various slicing directions; the coloured series (lines) of poles intersect at (next to) the sources.

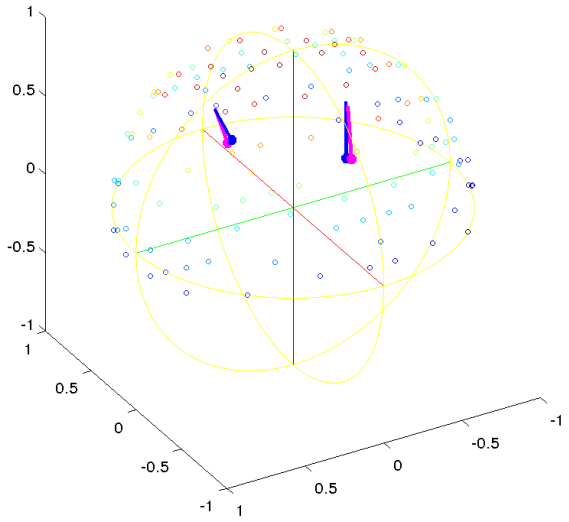

Figure 8: $K = 2$ actual and estimated sources and moment, spherical geometry.

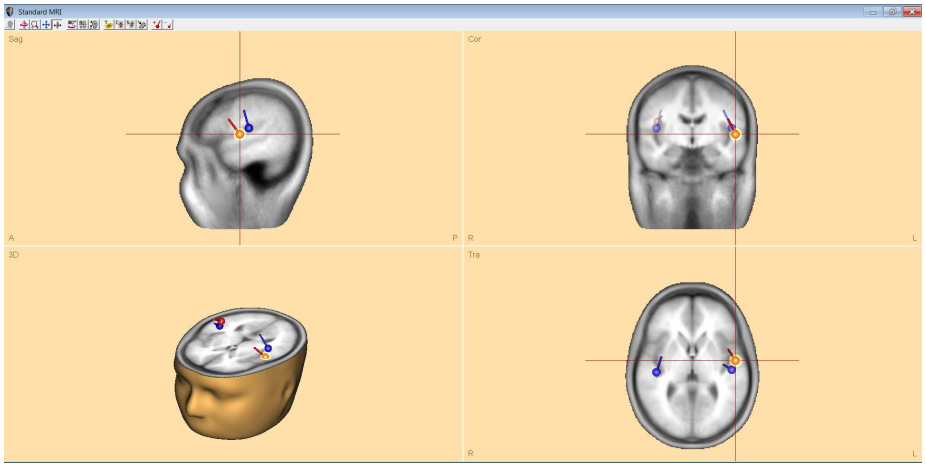

Figure 9: $K = 2$ actual and estimated sources and moments, realistic geometry, with the courtesy of BESA GmbH.

optimal location of the support of its support.

Acknowledgements: Many thanks to my main collaborators for this work: L. Baratchart (INRIA Sophia Antipolis, Team APICS), M. Clerc (INRIA S.A., Team ATHENA), T. Jordanov (BESA GmbH), J.-P. Marmorat (Mines ParisTech, CMA, S. A.), T. Papadopoulo (INRIA S.A., Team ATHENA).

References

[1] G. Alessandrini, L. Rondi, E. Rosset, S. Vessella, The stability for the Cauchy problem for elliptic equations, Inverse Problems, 25, 123004 (2009).

[2] B. Atfeh, L. Baratchart, J. Leblond, J.R. Partington, Bounded extremal and Cauchy-Laplace problems on the sphere and shell, J. Fourier Analysis& Applications, 16, 177-203 (2010).

[3] L. Baratchart, J. Leblond, J.-P. Marmorat, Inverse source problem in a 3D ball from best meromorphic approximation on 2D slices, Elec. Trans. Num. Anal. (2006).

[4] L. Baratchart, J. Leblond, J.R. Partington, N. Torkhani, Robust identification in the disc algebra from band-limited data, IEEE Trans. Automatic Control, 42 (1997).

[5] L. Baratchart, M. Olivi, F. Wielonsky, On a rational approximation problem in the real Hardy space H_2, Theoretical Computer Science, 94, 175–197 (1992).

[6] L. Baratchart, H. Stahl, M. Yattselev, Weighted extremal domains and rational approximation, Advances in Maths, 229, 357 407 (2012).

[7] G. Chen, J. Zhou, Boundary elements methods, Academic Press (1992).

[8] M. Clerc, J. Leblond, J.-P. Marmorat, T. Papadopoulo, Source localization in EEG using rational approximation on plane sections, Inverse Problems, 28, 055018 (2012).

[9] R. Dautray, J.-L. Lions, Analyse mathématique et calcul numérique pour les sciences er les techniques, vol. 2, Masson (1987).

[10] A. El Badia, T. Ha Duong, An inverse source problem in potential analysis, Inverse Problems, 16, 651–663 (2000).

[11] M. Clerc, J. Leblond, J.-P. Marmorat, T. Papadopoulo, Software FindSources3D, http://www-sop.inria.fr/apics/FindSources3D/

[12] V. Isakov, Inverse problems for partial differential equations, Applied Mathematical Sciences, vol. 127, Springer (1998).

[13] J.D. Jackson, Classical Electrodynamics, Wiley & sons (1998).

[14] D. Kandaswamy, T. Blu, D. Van De Ville, Analytic sensing: Noniterative retrieval of point sources from boundary measurements, SIAM J. Scientific Computing, 31 (2009).

[15] J. Kybic, M. Clerc, T. Abboud, O. Faugeras, R. Keriven, T. Papadopoulo, A common formalism for the integral formulations of the forward EEG problem, IEEE Trans. Medical Imaging, 24, 12–28 (2005).

[16] M. Scherg, T. Bast, P. Berg, Multiple source analysis of interictal spikes: goals, requirements, clinical value, J. of Clinical Neurophysiology, 16, 214–238 (1999).

[17] M. Tucsnak, G. Weiss, Observation and Control for Operator Semigroups, Birkhäuser (2009).

[18] S. Vessella, Locations and strengths of point sources: stability estimates, Inverse Problems, 8 (1992).

[19] M. Zghal, Problèmes inverses pour l'équation de Laplace en dimension 3, application l'EEG, PhD thesis, ENIT, Univ. Tunis El Manar (2010).